ISSN 1070-3284, Russian Journal of Coordination Chemistry, 2023, Vol. 49, No. 11, pp. 743–752. © Pleiades Publishing, Ltd., 2023.
Russian Text © The Author(s), 2023, published in Koordinatsionnaya Khimiya, 2023, Vol. 49, No. 11, pp. 719–728.

# Complexes of Silver 1,1,1,5,5,6,6,6-Octafluorohexane-2,4-dionate with π-Donor Ligands: Synthesis, Structure, and Thermal Properties

**E. S. Vikulova[a], *, I. Yu. Il'in[a], T. S. Sukhikh[a], P. K. Artamonova[b], and N. B. Morozova[a]**

[a] *Nikolaev Institute of Inorganic Chemistry, Siberian Branch, Russian Academy of Sciences, Novosibirsk, Russia*

[b] *Novosibirsk State Technical University, Novosibirsk, Russia*

**e-mail: lazorevka@mail.ru*

Received December 28, 2022; revised February 21, 2023; accepted March 13, 2023

**Abstract**—Two new Ag(I) complexes with 1,1,1,5,5,6,6,6-octafluorohexane-2,4-dionate ion (Ofhac) and π-donor neutral ligands, vinyltriethylsilane (VTES) or cycloocta-1,5-diene (COD), were synthesized with the goal to expand the library of silver precursors for chemical vapor deposition. The products were characterized by elemental analysis and IR and NMR spectroscopy. The complex [Ag(VTES)(Ofhac)] (**I**) was liquid under standard conditions; the temperature of its crystallization was below −20°C. Treatment of **I** with benzene gave rise to crystals of $[Ag_4(C_6H_6)_2(Ofhac)_4]_\infty$ (**II**), which was confirmed by NMR and X-ray diffraction (CCDC no. 2232810). The structure of $[Ag(COD)(Ofhac)]_2$ (**III**) was established by X-ray diffraction (CCDC no. 2232809). The binuclear molecules are formed due to the $\mu_2$-$\kappa^1$(O):$\kappa^1$(O') function of the Ofhac ligands (Ag–O, 2.458(2)–2.461(2) Å), while COD is $\kappa^2$-$\eta^2$:$\eta^2$-coordinated (Ag–C, 2.420(17)–2.684(11) Å). The thermal properties of **I** and **III** in comparison with analogues containing 1,1,1,5,5,5-hexafluoropentane-2,4-dionate ion (Hfac) were studied by thermogravimetry.

**Keywords:** silver, β-diketonate, cycloocta-1,5-diene, vinyltriethylsilane, X-ray diffraction, thermogravimetry

**DOI:** 10.1134/S1070328423600407

## INTRODUCTION

The interest in the preparation of Ag films and nanoparticles by chemical vapor deposition (MOCVD) or atomic layer deposition (ALD) has increased in the last decades [1–3]. This is due to the broad capabilities of these methods, which include precision control of characteristics of the resulting materials (composition, nanoparticle or grain size, and coating thickness and microstructure), and to the need to deposit Ag to non-planar substrates. For example, silver is considered to be an alternative to copper and aluminum for interconnectors in semiconductor devices, the miniaturization of which results in the fabrication of complex three-dimensional structures with a high aspect ratio [4]. A conformal coating of fibers and ordered arrays of silicon nanopillars by a thin Ag layer is of interest for optical applications [4, 5]. Apart from the non-planar geometry of the real substrates, the application of silver as an antibacterial agent for medical implants [2, 6, 7] brings about the challenge of formation of Ag nanoparticles and films on non-conductive [7, 8] or porous [9] materials, and predeposited Ti/TiO2 nanostructures [10, 11], including nanotubes, nanoneedles, etc.

However, the progress in MOCVD and ALD of silver-containing materials is markedly held up by very narrow range of silver compounds (precursors) that can be used in these processes [2]. The main problems are low thermal stability and polymeric structure of Ag(I) complexes with anionic ligands (β-diketonates, carboxylates) traditional for MOCVD/ALD precursors, which accounts for their low volatility. In order to form low-nuclearity complexes, different-ligand complexation, consisting in addition of a neutral ligand to saturate the silver coordination sphere, is actively used. A large set of N-, P-, O-, S-, and π-donor molecules with denticity from one to four have been tested as these additional ligands [2, 12–14].

Meanwhile, the effect of an anionic ligand on the properties of Ag(I) different-ligand complexes (DLCs) has been considered in detail only for carboxylate ions [2, 15–17]. Among β-diketonates (RCOCHCOR'), complexes of the 1,1,1,5,5,5-hexafluoropentane-2,4-dionate ion (R = R' = $CF_3$, Hfac) are most popular [2, 13, 14]. Different-ligand silver complexes with the 6,6,7,7,8,8,8-heptafluoro-2,2-dimethyloctane-3,5-dionate anion (R = $C_3F_7$, R' = $^t$Bu, Fod) containing bulky terminal substituents have also found use [2]. Previously, it was shown that barium complexes, which also bring about an oligomerization problem, with 1,1,1,5,5,6,6,6-octafluorohexane-2,4-dionate ion (R = $CF_3$, R' = $C_2F_5$, Ofhac) have a better volatility and thermal stability than the corresponding Hfac or Fod derivatives [18].

The goal of this study is to use the Ofhac ligand to prepare volatile Ag(I) DLCs and elucidate the effect of growing perfluoroalkyl chain in β-diketonate (R = $CF_3 \rightarrow C_2F_5$, Hfac vs. Ofhac) on their structure and thermal properties. As neutral ligands, we chose π-donor molecules, vinyltriethylsilane (VTES) and cycloocta-1,5-diene (COD), which differ in hapticity. The corresponding DLCs based on Ag(Hfac) differed in the physical state under ambient conditions (liquid [19] and solid [20], respectively) and have been successfully used for MOCVD and/or ALD at relatively low temperatures (≤280°C) [2]. Thus, the synthesis and investigation of new DLCs of the above types with improved thermal characteristics would expand the library of silver precursors for chemical vapor deposition processes.

## EXPERIMENTAL

The known complexes [Ag(VTES)(Hfac)] (**Ia**) and $[Ag(COD)(Hfac)]_2$ (**IIIa**) were synthesized by reported procedures ([19] and [21], respectively), which were modified to prepare the new compounds. The reaction vessels were protected from light using aluminum foil. The silver sources were $AgNO_3$ (99.9%, MZTsM-VTORMET) and $Ag_2O$. The oxide was obtained by usual neutralization procedure of the nitrate [22]. The sources of ligands, β-diketones HHfac and HOfhac (>99%), COD (99%, DALCHEM), and VTES (97%, Alfa Aesar), were used as received. $^1$H NMR spectrum of the initial VTES in $CDCl_3$ (δ, ppm): 6.10 dd, $J_{1,\,H-H}$ = 20.0 Hz, $J_{2,\,H-H}$ = 15.0 Hz, 1H ($CH_2$=C(H)–$SiEt_3$), 6.01 dd, $J_{1,\,H-H}$ = 15.0 Hz, $J_{2,\,H-H}$ = 4.4 Hz, 1H ($CH_2$=C(H)–$SiEt_3$), 5.69 dd, $J_{1,\,H-H}$ = 20.0 Hz, $J_{2,\,H-H}$ = 4.4 Hz, 1H ($CH_2$=C(H)$SiEt_3$), 0.96 t, $J_{H-H}$ = 7.9 Hz, 9H ($CH_3$), 0.6 q, $J_{H-H}$ = 7.9 Hz, 6H, ($CH_2$). The potassium salts of β-diketones K(L) were prepared by the standard neutralization reaction [23]. The solvents used to synthesize VTES complexes and $CDCl_3$ were degassed in an inert atmosphere prior to use.

**[Ag(VTES)(Ofhac)] (I)** was synthesized in an Ar atmosphere using Schlenk lines. VTES (0.14 mL, 0.105 g, 0.74 mmol) was added with stirring to a suspension of $Ag_2O$ (0.085 g, 0.37 mmol) in diethyl ether (15 mL), and the mixture was kept for 10 min. Then HOfhac (0.132 mL, 0.19 g, 0.74 mmol) was added, and the dark precipitate started to dissolve. The reaction mixture was kept for 24 h and concentrated to dryness, hexane (10 mL) was added, and the unreacted precipitate was separated on a glass porous filter. After concentration, a colorless liquid was formed. The yield was 86%.

IR (ν, $cm^{-1}$): 2961, 2920, 2885, 2885 $\nu_{s\,+\,as}$(C–H), 1672, 1643 ν(C=O), 1514, 1487 ν(C=C) + δ(C–H), 1331, 1304 $\nu_{as}$(C–F), 1196, 1145 $\nu_s$(C–F)+ ν(C–C), 795 ν(C–Si), 663 ν(Ag–O).

$^1$H NMR (δ, ppm): 6.00 (dd, $J_{1,\,H-H}$ = 18.2 Hz, $J_{2,\,H-H}$ = 13.8 Hz, 1H, $CH_2$=C(H)–$SiEt_3$), 5.96 (s, 1H, CH, Ofhac), 5.94 (dd, $J_{1,\,H-H}$ = 13.8 Hz, $J_{2,\,H-H}$ = 5.2 Hz, 1H, $CH_2$=C(H)–$SiEt_3$), 5.56 (dd, $J_{1,\,H-H}$ = 18.2 Hz, $J_{2,\,H-H}$ = 5.2 Hz, 1H, $CH_2$=C(H)$SiEt_3$), 1.00 (t, $J_{H-H}$ = 7.9 Hz, 9H, $CH_3$, VTES), 0.72 (q, $J_{H-H}$ = 7.9 Hz, 6H, $CH_2$, VTES). $^{13}$C{$^1$H} NMR (δ, ppm): 179.71 (t, $J_{F-C}$ = 23.4 Hz, $CF_3$–CO, Ofhac), 177.90 (q, $J_{F-C}$ = 32.8 Hz, $CF_2$–CO, Ofhac), 122.24 (s, $CH_2$=C(H)–$SiEt_3$), 119.6 (qt, $J_{1,\,F-C}$ = 287.5 Hz, $J_{2,\,F-C}$ = 36.1 Hz, $CF_3$–$CF_2$, Ofhac), 117.72 (q, $J_{F-C}$ = 288.2 Hz, $CF_3$, Ofhac), 108.24 (tq, $J_{1,\,F-C}$ = 226.4 Hz, $J_{2,\,F-C}$ = 37.3 Hz, $CF_3$–$CF_2$, Ofhac), 112.9 (s, $CH_2$=C(H)–$SiEt_3$), 89.08 (s, CH, Ofhac), 7.26 (s, $CH_3$, VTES), 3.51 (s, $CH_2$, VTES).

For $C_{14}H_{49}O_2FSiAg$

| | | | |
|---|---|---|---|
| Anal. calcd., % | C, 33.3 | H, 3.8 | F, 30.0 |
| Found, % | C, 33.3 | H, 3.9 | F, 29.9 |

**$[Ag_4(C_6H_6)(Ofhac)_4]_\infty$ (II)** was synthesized by dissolving the [Ag(VTES)(Ofhac)] complex in the Schlenk vessel in benzene followed by concentration and washing the resulting precipitate with hexane. The yield was 80%. $^1$H NMR (δ, ppm): 7.51 (s, 6H, $C_6H_6$), 6.00 (s, 2 × 1H, CH, Ofhac). $^{13}$C{$^1$H} NMR (δ, ppm): 180.22 (t, $J_{F-C}$ = 23.0 Hz, $CF_3$–CO, Ofhac), 177.90 (q, $J_{F-C}$ = 32.9 Hz, $CF_2$–CO, Ofhac), 127.02 (s, $C_6H_6$), 118.53 (qt, $J_{1,\,F-C}$ = 287.6 Hz, $J_{2,\,F-C}$ = 35.8 Hz, $CF_3$–$CF_2$, Ofhac), 117.62 q, $J_{F-C}$ = 288.0 Hz ($CF_3$, Ofhac), 108.20 (tq, $J_{1,\,F-C}$ = 226.0 Hz, $J_{2,\,F-C}$ = 37.9 Hz, $CF_3$–$CF_2$, Ofhac), 89.42 (s, CH, Ofhac).

The crystals of **II** suitable for X-ray diffraction were formed as a solution of **I** was kept in benzene at 0°C.

**$[Ag(COD)(Ofhac)]_2$ (III)** was synthesized in air under ambient conditions. COD (0.12 mL, 0.110 g, 1.0 mmol) was added to a solution of $AgNO_3$ (0.172 g, 1.0 mmol) in water (4 mL). The mixture was stirred for 30 min, and a solution of K(Ofhac) (0.300 g, 1.0 mmol) in water (2 mL) was added. A white precipitate was immediately formed. The reaction mixture was stirred for 30 min, then the precipitate was collected on a glass porous filter, washed with water, and dried in vacuum. The yield was 76%.

IR (ν, $cm^{-1}$): 3012, 2932, 2898 $\nu_{s+as}$(C–H), 1669, 1657 ν(C=O), 1518 ν(C=C) + δ(C–H), 1334, 1300 $\nu_{as}$(C–F), 1201, 1144 $\nu_s$(C–F) + ν(C–C), 664 ν(Ag–O).

$^1$H NMR (δ, ppm): 6.07 (s, 4H, CH, COD), 5.86 (s, 1H, CH, Ofhac), 2.52 (s, 8H, $CH_2$, COD).

For $C_{13}H_{13}O_2F_8Ag$

| | | | |
|---|---|---|---|
| Anal. calcd., % | C, 35.5 | H, 2.8 | F, 32.1 |
| Found, % | C, 35.9 | H, 2.8 | F, 32.2 |

The crystals of **III** suitable for X-ray diffraction were obtained by slow evaporation of a solution of **III** in toluene at −5°C.

Elemental analysis of samples for C and H was performed on a Euro EA3000 analyzer [24], and F was quantified using a Cary-60 spectrophotometer [25]. The standard error was not more than 0.5 wt %. IR spectra of samples as KBr pellets (**III**, **IIIa**) and as drops between KBr glasses (**I** and **Ia**) were measured on a Scimitar FTS 2000 spectrometer in the 4000–400 $cm^{-1}$ wavelength range. The absorption bands were assigned resorting to published data [26, 27]. The NMR spectra of solutions of new complexes **I** ($^1H$, $^{13}C\{^1H\}$) and **III** ($^1H$) in $CDCl_3$ were measured on a Bruker Avance 500 Plus spectrometer ($^1H$: 500.129 MHz, $^{13}C$: 125.757 MHz) at 25°C. The chemical shifts (δ, ppm) were referred to the residual proton signals in $CDCl_3$ ($^1H$ = 7.26; $^{13}C$ = 77.16) as the internal standard [28].

**Single-crystal X-ray diffraction** study of compounds **II** and **III** was carried out at the Center for Collective Use of the Nikolaev Institute of Inorganic Chemistry, Siberian Branch, Russian Academy of Sciences, using a Bruker D8 Venture diffractometer with a CMOS PHOTON III detector and an IμS 3.0 microfocus X-ray source (Mo$K_\alpha$ radiation, λ = 0.71073 Å, Montel focusing mirrors). The crystal structures were solved using SHELXT software [29] and refined by means of SHELXL software [30] with the OLEX2 graphical interface [31]. In the case of **III**, the atomic displacement parameters for non-hydrogen atoms were refined anisotropically. The atoms of COD and the $C_2F_5$ moiety are disordered over two sites with occupancies of 58/42 and 51/49, respectively. For these groups, constraints were imposed on the bond lengths and angular distances and some constraints were imposed on atomic displacement parameters. The hydrogen atoms were located geometrically. In the case of compound **II**, the X-ray diffraction pattern showed pronounced diffuse scattering along *a**, indicating the presence of faults of crystal packing; as a result, we were unable to attain good agreement between the structural model and the experiment. Only Ag and O atoms and benzene C atoms were located reliably during the structure solution. The other atoms were introduced nominally with geometry constraints for the Ofhac moieties. The Ag atoms were refined in the anisotropic approximation; the other atoms were characterized by constant atomic displacement parameters: $U_{iso}$ = 0.15. The crystallographic characteristics of **I** are summarized in Table 1.

The full set of X-ray diffraction parameters for **II** and **III** is deposited with the Cambridge Crystallographic Data Centre (no. 2232809 and 2232810, respectively); http://www.ccdc.cam.ac.uk.

The thermal properties of the complexes were studied by thermogravimetry (TG). The weight loss and differential thermal analysis (DTA) curves were measured on a Netzsch TG 209 F1 Iris thermobalance in a helium atmosphere (30 mL $min^{-1}$) at a heating rate of 10°C $min^{-1}$ for 10 ± 1 mg samples placed into an open Al crucible.

## RESULTS AND DISCUSSION

Silver (I) β-diketonate complexes with VTES ligands (**I** and **Ia**) were assembled in situ from $Ag_2O$, alkene, and β-diketone in an organic solvent under inert atmosphere [19]. A similar approach was also proposed previously for cyclooctadienyl complexes [20]; however, a more convenient method is the reaction of Ag(COD)($NO_3$) with the β-diketone salt [21], which gives target products under ambient conditions in an aqueous solution.

The physical state of new Ag(I) complexes with the Ofhac ligand (**I**, **III**) is the same as that for their Hfac analogues (**Ia**, **IIIa**): compounds containing COD are solids, while the introduction of VTES results in a considerable decrease in the melting point (the compounds are liquid at room temperature). In the IR spectra of **I** and **III**, characteristic absorption bands corresponding to vibrations of the Ofhac moieties (ν(C=O), ν(C=C), $\nu_{as}$(C–F), $\nu_s$(C–F)) are located closely. Note a strong absorption band at 664 $cm^{-1}$ for the ν(Ag–O) stretching mode. The intensity of bands corresponding to the C–H stretching modes is much higher for complexes **I** and **Ia** than for **III** and **IIIa**, because of the presence of ethyl groups in the VTES ligand.

For complex **III**, it was possible to obtain crystals suitable for X-ray diffraction. The $^1H$ NMR spectrum for **III** is in line with the stoichiometry of $[Ag(COD)(Ofhac)]_2$; the set of signals is similar to that for **IIIa** [20]. No signals corresponding to uncoordinated COD or HOfhac are observed. The signals of the cyclooctadiene olefin groups in the spectrum of **III** are shifted downfield by 0.49 ppm in comparison with those of free COD.

A long-term cooling of VTES complex **I** (−20°C) did not result in the formation of crystals. Therefore, the composition of **I** was confirmed by extensive characterization using $^1H$ and $^{13}C\{^1H\}$ NMR spectroscopy. The spectra of **I** are consistent with the formula [Ag(VTES)(Ofhac)]; the set of signals is similar to that for **Ia** [19]. No signals corresponding to uncoordinated VTES or HOfhac are present. Similarly to the related complexes of Hfac and Tfac (Tfac = 1,1,1-trifluoropentane-2,4-dionate ion) [19], in the $^1H$ NMR spectrum of **I**, the olefin proton signals are shifted upfield. However, the difference is only about 0.1 ppm, whereas for L = Hfac or Tfac, it is much greater (~1 ppm). This distinction can be due to the relatively weaker bond of silver with the alkene, as confirmed by the reaction of **I** with benzene.

**Table 1.** Crystallographic characteristics and structure refinement details for $[Ag(COD)(Ofhac)]_2$ (**III**) and $[Ag_4(C_6H_6)_2(Ofhac)_4]_\infty$ (**II**)

| Parameter | Value | |
|---|---|---|
| | **III** | **II** |
| Molecular formula | $C_{28}H_{26}O_4F_{16}Ag_2$ | $C_{18}H_8O_4F_{16}Ag_2$ |
| $M$ | 946.23 | 807.98 |
| Temperature, $K$ | 150(2) | 150(2) |
| Space group | $P2_1/c$ | $C2/c$ |
| $a$, Å | 10.4763(4) | 23.5652(8) |
| $b$, Å | 14.4048(5) | 12.6173(4) |
| $c$, Å | 10.7816(4) | 16.6051(6) |
| β, deg | 94.0960(10) | 108.6390(10) |
| $V$, Å$^3$ | 1622.88(10) | 4678.2(3) |
| $Z$ | 2 | 8 |
| ρ(calcd.), g/cm$^3$ | 1.936 | 2.294 |
| μ, mm$^{-1}$ | 1.332 | 1.827 |
| $F$(000) | 928.0 | 3088.0 |
| Crystal size, mm | 0.08 × 0.06 × 0.02 | 0.38 × 0.23 × 0.16 |
| Data collection range of 2θ, deg | 4.726–52.744 | 3.648–48.862 |
| Ranges of $h$, $k$, $l$ | $-13 \le h \le 13$,<br>$-17 \le k \le 18$,<br>$-13 \le l \le 13$ | $-27 \le h \le 27$,<br>$-14 \le k \le 14$,<br>$-19 \le l \le 19$ |
| Number of measured reflections | 17796 | 22002 |
| Number of unique reflections ($R_{int}$, $R_\sigma$) | 3320<br>(0.0330, 0.0238) | 3857<br>(0.0354, 0.0264) |
| Number of data/constraints/refined parameters | 3320/226/363 | 3857/63/121 |
| GOOF on $F^2$ | 1.032 | 3.769 |
| $R$-factor ($I > 2\sigma(I)$) | $R_1 = 0.0300$,<br>$wR_2 = 0.0667$ | $R_1 = 0.2565$,<br>$wR_2 = 0.6784$ |
| $R$-factor (all data) | $R_1 = 0.0392$,<br>$wR_2 = 0.0726$ | $R_1 = 0.2803$,<br>$wR_2 = 0.7047$ |
| $\Delta\rho_{max}/\Delta\rho_{min}$, e/Å$^3$ | 0.75/–0.74 | 6.25/–3.21 |

In particular, the addition of benzene to **I** followed by concentration in vacuum and keeping the liquid residue at 0°C affords crystals of **II** that do not melt at room temperature. Having been washed with hexane, the crystals are completely soluble in $CDCl_3$. The signals for coordinated Ofhac (6.00 ppm for C–H; 180 and 178 ppm for C=O), which virtually coincide with similar signals for **I**, are retained in the NMR spectra. All signals corresponding to VTES disappear, while signals corresponding to benzene (7.36 and 127 ppm) appear. The proton signals are shifted downfield (0.15 ppm) with respect to those for free benzene [28], which attests to weak coordination of benzene to silver. The Ofhac : benzene ligand ratio is 2 : 1. The structure of the related complex with toluene with this stoichiometry, $[Ag_4(C_7H_6)_2(Hfac)_4]_\infty$, was proved by X-ray diffraction [32]. Thus, π-donor solvents can replace VTES in the Ag(I) coordination sphere. Apparently, the reactivity is determined by the anionic ligand: according to NMR data in $C_6D_6$, as opposed to **I**, no such replacement takes place for complexes with L = Hfac and Tfac containing no bulky groups [19].

Due to the poor quality of X-ray diffraction data for the crystals of **II**, we were unable to reliably determine the position of the β-diketonate ligand (L). Nevertheless, it was possible to locate Ag atoms and benzene, which suggested the structural organization similar to that of $[Ag_4(C_7H_6)_2(Hfac)_4]_\infty$ [32]. These compounds form a layered structure in which the {Ag(L)} building blocks are connected by the Ag–O bonds to form tetranuclear moieties, which are, in turn, linked by bridging benzene ligands to form layers (Scheme 1). A schematic view of the structure of $[Ag_4(C_6H_6)_2(Ofhac)_4]_\infty$ (**II**) and $[Ag_4(C_7H_6)_2(Hfac)_4]_\infty$ (**III**) is depicted in Scheme 1.

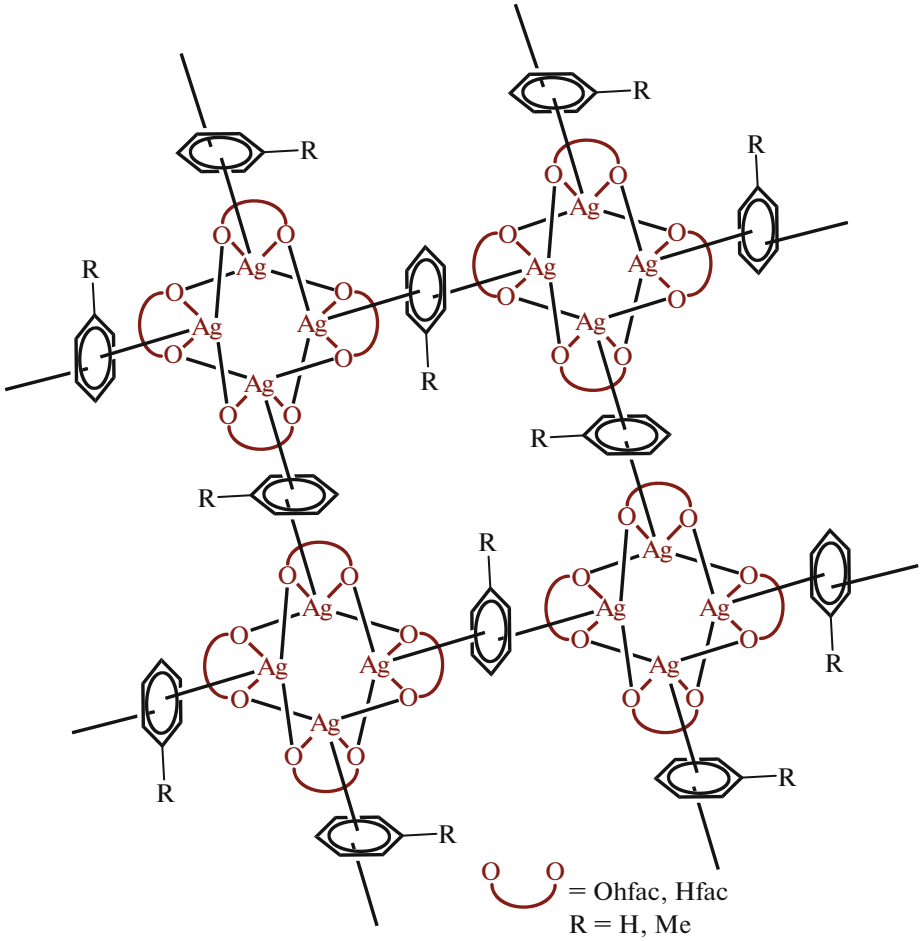


**Scheme 1.**

The elongated atomic displacement ellipsoids of silver attest to the disorder of structural groups caused by the disruption of crystal packing, which is manifested as diffuse scattering in the *a** direction in the diffraction pattern. The crystal metric in the *b* and *c* directions for the crystals of **II** is close to the corresponding metric for $[Ag_4(C_7H_6)_2(Hfac)_4]_\infty$ [32], indicating that the layer structures in these compounds are similar. The layer packing along the third axis (*a*) is somewhat different as a result of greater displacement of the layers relative to one another in **II**. In addition, the layer packing along the *a* axis in **II** has a simpler order: every second layer in **II** is translationally equivalent, while in $[Ag_4(C_7H_6)_2(Hfac)_4]_\infty$ [32], every fourth layer is equivalent.

According to X-ray diffraction data, the coordination environment of the silver atom in the centrosymmetric binuclear complex **III** is formed by $\kappa^2$-$\eta^2$:$\eta^2$-cyclooctadiene (the Ag–$C_{COD}$ distances are in the range of 2.420(17)–2.684(11) Å) and two β-diketonate ions, which perform the $\mu_2$-$\kappa^1$(O):$\kappa^1$(O')-bridging function (Fig. 1). The corresponding Ag–O distances are 2.458(2) and 2.461(2) Å; the Ag···O contacts with longer distances of 2.601(2) and 2.715(2) Å are also present. Thus, the coordination polyhedron of silver is the distorted $AgC^*_2O_2$ tetrahedron (C* is the the midpoint of the COD π-bond). The conjugated part of the β-diketonate ligand is planar: the folding angle of the CC line is 0.8°. The angle between the $\{C_3O_2\}$ and {OAgO} planes is 42.3°. The distance between the silver atoms in the binuclear molecule is 2.9199(5) Å,

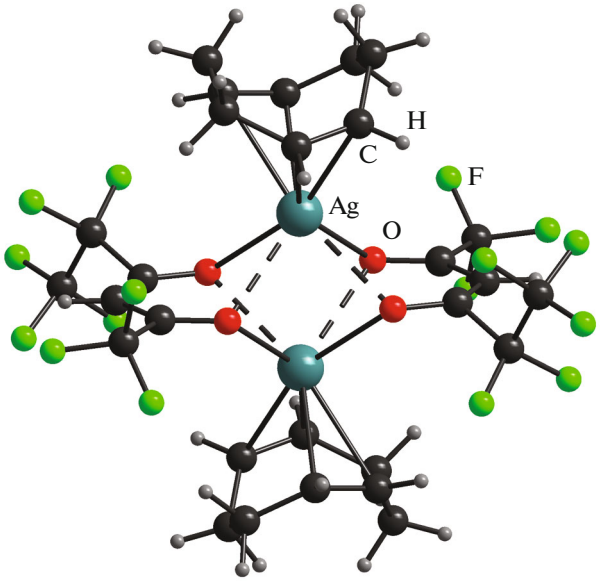


**Fig. 1.** Structure of the $[Ag(COD)(Ofhac)]_2$ molecule (**III**). The short Ag···O contacts are shown by dashed lines.

which falls in the range most typical of argentophilic contacts (2.9–3.1 Å, [33]).

It is noteworthy that the structure of molecule **III** is similar to the structures of previously described complexes with the Hfac anion or COD (**IIIa**) [20] or its methylated derivative (1,5-dimethylcycloocta-1,5-diene) [34]. In the last-mentioned study, it was shown that characteristics of the silver environment in this binuclear molecule are virtually independent of the measurement temperature. This makes it possible to evaluate the effect of replacement of the β-diketonate ligand in $[Ag(COD)(L)]_2$ (L = Hfac in **IIIa**, Ofhac in **III**). The average Ag–$C_{COD}$ distances virtually coincide (2.55(6) Å for L = Hfac). The average Ag–O distances are comparable; however, in the case of **IIIa**, one Hfac ligand has a $\mu_2$-$\kappa^2$(O,O'):$\kappa^2$(O,O')-bridging position, while the second $\mu_2$-$\kappa^1$(O):$\kappa^1$(O') anion has markedly elongated Ag···O contacts (2.644(3) and 2.793(2) Å) similar to those in **III**. The distance between the silver atoms in **IIIa** is ~0.03 Å longer than that in **III**. Thus, the elongation of the fluoroalkyl chain resulted in unification of the coordination role of ligands in the binuclear molecule. Presumably, the elongated distances to Ag for L = Ofhac would facilitate the formation of mononuclear molecules upon transfer to the gas phase.

In the structure of **III**, the COD and Ofhac ligands are disordered over two distinct positions with similar occupancies. Thus, there are four options for the position of the molecule with different ligand arrangements (if only centrosymmetric molecules are considered). In order to find out whether there are clear steric restrictions to the potential implementation of these options, we analyzed the Hirshfeld surfaces. The designations for types of COD (C(1) or C(2)) and for two Ofhac (F(1) and F(2)) molecules were introduced; the corresponding molecules would be C(1)F(1), C(1)F(2), C(2)F(1), and C(2)F(2). This is exemplified in Fig. 2, which shows the C(1)F(1) and C(2)F(1) molecules. Analysis of the Hirshfeld surfaces did not reveal any steric restrictions for these types of molecules. There are weak intermolecular F···F and F···H contacts with the shortest distances of 3.12 and 2.38 Å, respectively. The H···F contacts are shorter for the molecule with C(2) than for the molecule with C(1) (Table 2). Since both C(1) and C(2) type molecules are present in the crystal, these shorter contacts do not play a considerable role in the molecular packing. Similar analysis of the intermolecular contacts for non-centrosymmetrical types of the crystal packing did not reveal noticeable steric restrictions either. In the case of Hfac-based analogue (**IIIa**), pronounced disorder of the $CF_3$ groups was mentioned without further details [20]; therefore, analysis of the Hirshfeld surfaces was not carried out for this structure.

In the crystals of $[Ag(COD)(L)]_2$ (L = Hfac in **IIIa**, Ofhac in **III**), one can distinguish layers (in the *bc* and *ba* planes, respectively) in which the molecules are packed in the same way (Figs. 3a, 3b). Intermolecular van der Waals interactions between COD atoms occur in the layers, while the $CF_3$ or $C_2F_5$ groups protrude out of the planes. The packings of the layers are different. Indeed, in **IIIa**, two Hfac moieties of neigh-

**Table 2.** Intermolecular F···H distances in the 2.30–2.60 Å range for four types (C(1)F(1), C(1)F(2), C(2)F(1), and C(2)F(2)) of molecules of $[Ag(COD)(Ofhac)]_2$ (**III***)

| C(1)F(1) | | C(1)F(2) | | C(2)F(1) | | C(2)F(2) | |
|---|---|---|---|---|---|---|---|
| F(7A)···H(14B)[1] | 2.51 | F(5)···H(14A)[2] | 2.53 | F(1)···H(10C)[3] | 2.38 | F(1)···H(10C)[3] | 2.38 |
| F(5A)···H(15B)[2] | 2.57 | | | F(4A)···H(9A)[4] | 2.50 | F(8)···H(15C)[6] | 2.47 |
| F(8A)···H(11A)[1] | 2.58 | | | F(4A)···H(16A)[5] | 2.53 | F(8)···H(16A)[5] | 2.53 |
| F(8A)···H(14B)[1] | 2.60 | | | | | F(7)···H(10D)[6] | 2.58 |
| | | | | | | F(7)···H(9A)[4] | 2.59 |

* Symmetry codes: [1] $-x$, $0.5 - y$, $0.5 + z$; [2] $-1 - x$, $1 - y$, $1 - z$; [3] $-2 - x$, $0.5 + y$, $0.5 - z$; [4] $-2 - x$, $1 - y$, $1 - z$; [5] $-x$, $1.5 - y$, $0.5 + z$; [6] $-x$, $y$, $1 + z$.

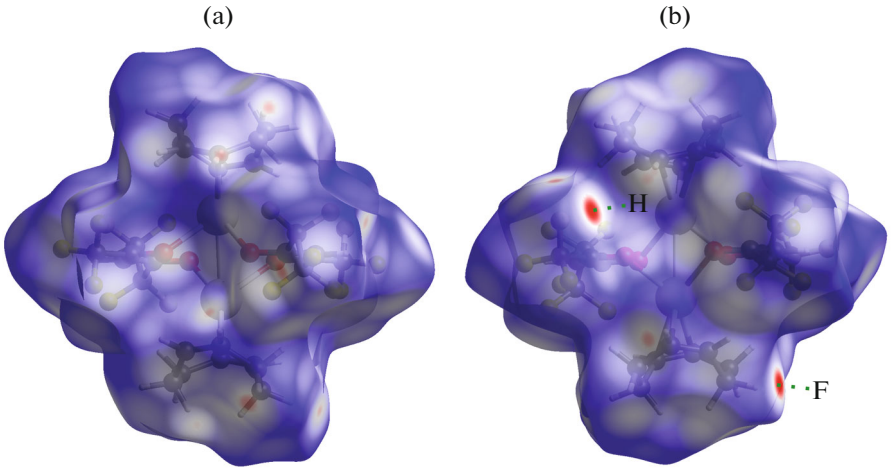


**Fig. 2.** Hirshfeld surfaces for two types of molecule of $[Ag(COD)(Ofhac)]_2$ (**III**): (a) C(1)F(1) and (b) C(2)F(1). Red color shows the regions in which the distance between atoms is shorter than the sum of their van der Waals radii; white color indicates the regions in which the distance is equal to the sum, and blue marks the regions where this distance is greater than the sum of the van der Waals radii. The differences between the distances range from –0.2 to 1.0 Å. For the shortest contacts (green dashed lines), the atoms of the neighboring molecule are indicated.

boring layers are located opposite to each other, with the distance between the planes consisting of atoms of these moieties being 1.1 Å (Fig. 3d). Meanwhile in **III**, due to the greater steric effect of the $C_2F_5$ group compared to $CF_3$, the β-diketonate moieties are considerably shifted relative to each other, and the distance between the planes may be as great as 4.5 Å (Fig. 3c).

The thermal properties of new complexes **I** and **III** and their Hfac analogues **Ia** and **IIIa** were studied by TG in an inert atmosphere (He flow, 10°/min, Fig. 4). According to DTA, the solid complexes $[Ag(COD)(L)]_2$ **III** and **IIIa** melt at temperatures of 76 and 110°C, respectively. The results for **IIIa** correspond to published data [35]; the results for **III** were confirmed by measurements on a Kofler hot stage. Thus, elongation of the fluorinated substituent in the β-diketonate ligand lowers the melting point of the complex. This trend also holds for [Ag(VTES)(L)]: liquid **Ia** (L = Hfac), unlike **I** (L = Ofhac), can be crystallized by keeping at –20°C. A pronounced endotherm at 54°C, probably corresponding to a solid-phase transformation, deserves attention in the DTA curve of **III**.

The major mass loss of the [Ag(VTES)(L)] complexes starts at 65°C (L = Ofhac, **I**) or 45°C (L = Hfac, **Ia**) and includes two overlapping stages (Fig. 4). The first one can be attributed to elimination of the neutral ligand. However, even for complex **Ia**, in which the stages are better separated, the weight loss at the inflection point (175°C) is 33.2%, which is slightly greater than the content of VTES (31.1%). This suggests partial evaporation of the complexes during the TGA experiment. This is also confirmed by the weight of the residue (exp), which is lower than the silver content (calcd.): 16.7% exp. (300°C) vs. 21.3% calcd. for **I** and 22.1% (310°C) vs. 23.6% cacld. for **Ia**. The more pronounced difference between the values attests to a more efficient evaporation of the new complex **I**. If the expected decomposition product is pure silver metal, it can be estimated that approximately 20% of the complex has evaporated for **I** and approximately 6% has evaporated for **Ia**.

The major weight loss of **III** and **IIIa** starts at their melting points, includes one stage, and ends at ~260°C (Fig. 4). This is followed by slow monotonic decrease in the sample weight, which can be attributed to the thermal after-burning of carbon-containing products of ligand decomposition. Indeed, decomposition of **IIIa** to silver metal under inert atmosphere was reported previously [35]. In our experiments, the final residual weights (460°C, start of the constant weight regions) of both complexes is somewhat below the silver content: 21.3% exp. vs. 22.8% calcd. for **III** and 24.6% exp. vs. 25.5% calcd. for **IIIa**. A large difference is also observed for the complex with the Ofhac ligand. The weight loss curve for **III** is shifted to lower temperature (by ~10°C), which may also indicate its relatively higher volatility.

It is noteworthy that the predominance of decomposition over evaporation in TGA experiments at atmospheric pressure is typical of silver complexes used in chemical vapor processes; furthermore, decomposition in vacuum shows the opposite trend [36].

Thus, we prepared volatile silver complexes with the new β-diketonate ligand [Ag(VTES)(Ofhac)] (**I**) and $[Ag(COD)(Ofhac)]_2$ (**III**). The complexes were characterized by elemental analysis, IR and NMR spectroscopy, and TG analysis. The physical state of the new complexes under ambient conditions corre-

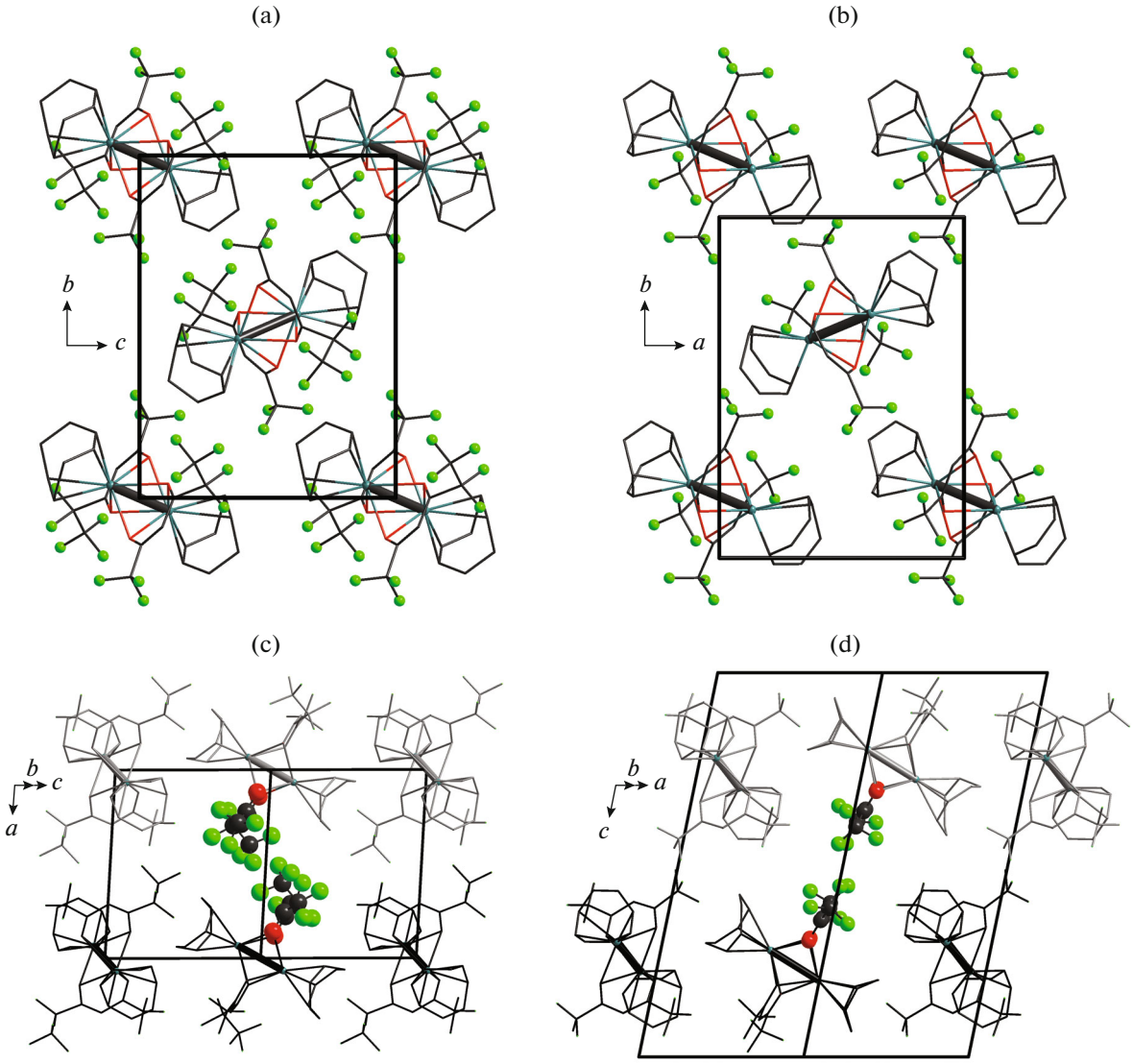


**Fig. 3.** Structure of the layer in $[Ag(COD)(L)]_2$, L = (a) Ofhac (**III**) and (b) Hfac (**IIIa**). The H atoms and the disorder are not shown. Relative positions of neighboring layers in the structures for L = (c) Ofhac and (d) Hfac. Different layers are highlighted in gray and black; the neighboring β-diketonate ligands for (c) and (d) are shown with the ball-and-stick model.

sponds to that of their known analogues: [Ag(VTES)(Hfac)] **Ia** (liquid) and $[Ag(COD)(Hfac)]_2$ **IIIa** (solid). An increase in the size of the fluorinated substituent (L = Hfac → Ofhac) decreases the melting points of compounds. According to X-ray diffraction data, this modification of the ligand leads to unification of its coordination function in the binuclear $[Ag(COD)(L)]_2$ molecule with decreasing number of bridging bonds between silver atoms. The VTES ligand in **I** can be replaced by benzene to give $[Ag_4(C_6H_6)_2(Ofhac)_4]_\infty$, which was not observed for **Ia**. Complex **I** is thermally more stable, since it is characterized by a higher temperature of VTES elimination under atmospheric pressure. According to TG analysis, the new complexes **I** and **III** appear to be more volatile compared to analogues **Ia** and **IIIa**.

## ACKNOWLEDGMENTS

The authors wish to thank M.A. Kurykin (Nesmeyanov Instituted of Organoelement Compounds, Russian Academy of Sciences) for the synthesis of fluorinated β-diketones and S.A. Gulyaev (Novosibirsk State University; Nikolaev Institute of Inorganic Chemistry, Siberian Branch, Russian Academy of Sciences) for participation in the primary synthesis of $[Ag(COD)(Ofhac)]_2$. We are grateful to the Chemical Research Center for Collective Use, Siberian Branch, Russian Academy of Sciences (Vorozhtsov Novosibirsk Institute of Organic Chemistry, Siberian Branch, Russian Academy of Sciences) for conduction of the elemental analysis and to the Center for Collective Use of the Nikolaev Institute of Inorganic Chemistry, Siberian Branch, Russian Academy of Sciences, for the possibility to collect X-ray diffraction data. The authors

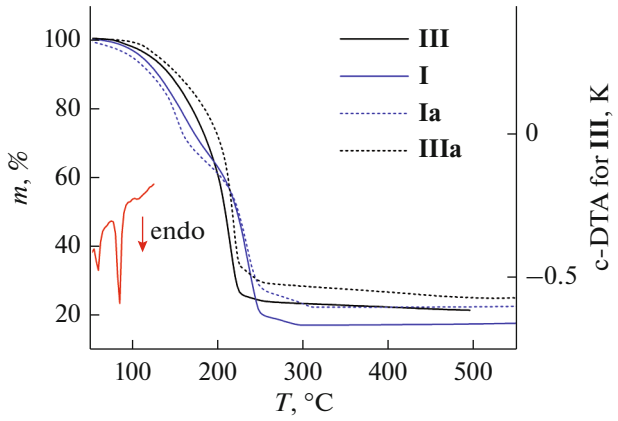


**Fig. 4.** Weight loss curves for [Ag(VTES)(L)] (L = Ofhac (**I**) Hfac (**Ia**)) and $[Ag(COD)(L)]_2$ (L = Ofhac (**III**), Hfac (**IIIa**)) and a part of DTA curve for **III**.

thank the Ministry of Science and Higher Education of the Russian Federation (Project nos. 121031700313-8 and 121031700314-5).

## FUNDING

This study was supported by a grant of President of the Russian Federation for the state support of young Russian scientists, Candidates of Sciences (MK-6148.2021.1.3).

## CONFLICT OF INTEREST

The author of this work declares that they has no conflicts of interest.

## REFERENCES

1. Leskelä, M., Ritala, M., and Nilsen, O., *MRS Bull.*, 2011, vol. 36, no. 11, p. 877. https://doi.org/10.1557/mrs.2011.240
2. Piszczek, P. and Radtke, A., in *Noble and Precious Metals—Properties, Nanoscale Effects and Applications*, Seehra, M.S. and Bristow, A.D., Eds., London: IntechOpen, 2018, p. 187. https://doi.org/10.5772/intechopen.71571
3. Hagen, D.J., Pemble, M.E., and Karppinen, M., *Appl. Phys. Rev.*, 2019, vol. 6, no. 4, p. 041309. https://doi.org/10.1063/1.5087759
4. Wack, S., Lunca Popa, P., Adjeroud, N., et al., *ACS Appl. Mater. Interfaces*, 2020, vol. 12, no. 32, p. 36329. https://doi.org/10.1021/acsami.0c08606
5. Mandia, D.J., Zhou, W., Albert, J., et al., *Chem. Vapor Depos.*, 2015, vol. 21, nos. 1–3, p. 4. https://doi.org/10.1002/cvde.201400059
6. Radtke, A., Grodzicka, M., Ehlert, M., et al., *J. Clin. Med.*, 2019, vol. 8, no. 3, p. 334. https://doi.org/10.3390/jcm8030334
7. Basova, T.V., Vikulova, E.S., Dorovskikh, S.I., et al., *Mater. Des.*, 2021, vol. 204, p. 109672. https://doi.org/10.1016/j.matdes.2021.109672
8. Liu, X., Gan, K., Liu, H., et al., *Dental Mater.*, 2017, vol. 33, no. 9, p. e348. https://doi.org/10.1016/j.dental.2017.06.014
9. Geng, H., Poologasundarampillai, G., Todd, N., et al., *ACS Appl. Mater. Interfaces*, 2017, vol. 9, no. 25, p. 21169. https://doi.org/10.1021/acsami.7b05150
10. Radtke, A., Jedrzejewski, T., Kozak, W., et al., *Nanomaterials*, 2017, vol. 7, no. 7, p. 193. https://doi.org/10.3390/nano7070193
11. Nazarov, D., Ezhov, I., Yudintceva, N., et al., *J. Funct. Biomater.*, 2022, vol. 13, no. 2, p. 62. https://doi.org/10.3390/jfb13020062
12. Zanotto, L., Benetollo, F., Natali, M., et al., *Chem. Vapor Depos.*, 2004, vol. 10, no. 4, p. 207. https://doi.org/10.1002/cvde.200306290
13. Mishra, S. and Daniele, S., *Chem. Rev.*, 2015, vol. 115, no. 16, p. 8379. https://doi.org/10.1021/cr400637c
14. Liu, H., Battiato, S., Pellegrino, A.L., et al., *Dalton Trans.*, 2017, vol. 46, no. 33, p. 10986. https://doi.org/10.1039/C7DT01647F
15. Grodzicki, A., Łakomska, I., Piszczek, P., et al., *Coord. Chem. Rev.*, 2005, vol. 249, nos. 21–22, p. 2232. https://doi.org/10.1016/j.ccr.2005.05.026
16. Szłyk, E., Szczęsny, R., and Wojtczak, A., *Dalton Trans.*, 2010, vol. 39, no. 7, p. 1039. https://doi.org/10.1039/B911741E
17. Madajska, K., Dobrzańska, L., Muzioł, T., et al., *Polyhedron*, 2022, vol. 227, p. 116149. https://doi.org/10.1016/j.poly.2022.116149
18. Sato, H. and Sugawara, S., *Inorg. Chem.*, 1993, vol. 32, no. 10, p. 1941. https://doi.org/10.1021/ic00062a011
19. Chi, K.M., Chen, K.H., Peng, S.M., et al., *Organometallics*, 1996, vol. 15, no. 10, p. 2575. https://doi.org/10.1021/om960013e
20. Bailey, A., Corbitt, T.S., Hampden-Smith, M.J., et al., *Polyhedron*, 1993, vol. 12, no. 14, p. 1785. https://doi.org/10.1016/S0277-5387(00)84613-6
21. Partenheimer, W. and Johnson, E.H., *Inorg. Chem.*, 1972, vol. 11, no. 11, p. 2840. https://doi.org/10.1021/ic50117a052
22. Karyakin, Yu.V. and Angelov, I.I. *Chistye khimicheskie veshchestva* (Pure Chemicals), Moscow: Khimiya, 1974.
23. Kochelakov, D.V., Vikulova, E.S., Kurat'eva, N.V., et al., *J. Struct. Chem.*, 2023, vol. 64, no. 1, p. 82.
24. Fadeeva, V.P., Tikhova, V.D., Deryabina, Y.M., et al., *J. Struct. Chem.*, 2014, vol. 55, no. 5, p. 972. https://doi.org/10.1134/S0022476614050278
25. Tikhova, V.D., Fadeeva, V.P., Nikulicheva, O.N., et al., *Chem. Sustain. Dev.* 2022, vol. 30, p. 640. https://doi.org/10.15372/CSD2022427
26. Gordon, A.J., and Ford, R.A., *The Chemist's Companion. A Handbook of Practical Data, Techniques, and References*, New York: Wiley, 1972.
27. Vikulova, E.S., Sukhikh, T.S., Gulyaev, S.A., et al., *Molecules*, 2022, vol. 27, no. 3, p. 677. https://doi.org/10.3390/molecules27030677

28. Fulmer, G.R., Miller, A.J.M., Sherden, N.H., et al., *Organometallics*, 2010, vol. 29, p. 2176. https://doi.org/10.1021/om100106e
29. Sheldrick, G.M., *Acta Crystallogr., Sect. A: Cryst. Adv.*, 2015, vol. 71, p. 3. https://doi.org/10.1107/S2053273314026370
30. Sheldrick, G., *Acta Crystallogr., Sect. C: Struct. Chem.*, 2015, vol. 71, p. 3. https://doi.org/10.1107/S2053229614024218
31. Dolomanov, O.V., Bourhis, L.J., Gildea, R.J., et al., *J. Appl. Crystallogr.*, 2009, vol. 42, p. 339. https://doi.org/10.1107/S0021889808042726
32. Evans, W.J., Giarikos, D.G., Josell, D., et al., *Inorg. Chem.*, 2003, vol. 42, no. 25, p. 8255. https://doi.org/10.1021/ic034649r
33. Schmidbaur, H. and Schier, A., *Angew. Chem.*, 2015, vol. 54, no. 3, p. 746. https://doi.org/10.1002/anie.201405936
34. Doppelt, P., Baum, T.H., and Ricard, L., *Inorg. Chem.*, 1996, vol. 35, no. 5, p. 1286. https://doi.org/10.1021/ic9410102
35. Black, K., Singh, J., Mehta, D., et al., *Sci. Rep.*, 2016, vol. 6, no. 1, p. 1. https://doi.org/10.1038/srep20814
36. Jurczyk, J., Glessi, C., Madajska, K., et al., *J. Therm. Anal. Calorim.*, 2022, vol. 147, no. 3, p. 2187. https://doi.org/10.1007/s10973-021-10616-6

*Translated by Z. Svitanko*